Scanning Microscopy

Volume 9 | Number 3 Article 3

9-5-1995

Imaging of Cherenkov and Transition Radiation from Thin Films and Particles

N. Yamamoto
Tokyo Institute of Technology

A. Toda
Tokyo Institute of Technology

Follow this and additional works at: https://digitalcommons.usu.edu/microscopy

Part of the Biology Commons

Recommended Citation

Yamamoto, N. and Toda, A. (1995) "Imaging of Cherenkov and Transition Radiation from Thin Films and Particles," *Scanning Microscopy*: Vol. 9 : No. 3 , Article 3.
Available at: https://digitalcommons.usu.edu/microscopy/vol9/iss3/3

This Article is brought to you for free and open access by the Western Dairy Center at DigitalCommons@USU. It has been accepted for inclusion in Scanning Microscopy by an authorized administrator of DigitalCommons@USU. For more information, please contact digitalcommons@usu.edu.

Scanning Microscopy, Vol. 9, No. 3, 1995 (Pages 669-676) 0891-7035/95$5.00+.25
Scanning Microscopy International, Chicago (AMF O'Hare), IL 60666 USA

IMAGING OF CHERENKOV AND TRANSITION RADIATION FROM THIN FILMS AND PARTICLES

N. Yamamoto* and A. Toda

Department of Physics, Tokyo Institute of Technology,
Oh-okayama, Meguro-ku, Tokyo 152, Japan

(Received for publication March 28, 1995 and in revised form September 5, 1995)

Abstract

Cherenkov radiation and transition radiation, which are generated by high energy electrons with constant velocity, can be detected in a transmission electron microscope using a cathodoluminescence (CL) detection system. The characteristic peaks due to interference were observed in the emission spectra from thin films of mica, silicon and silver, and their dependence on sample thickness and accelerating voltage was studied. Particles of $BaTiO_3$ and MgO also showed characteristic feature in the spectra which changed with their size. A recently developed imaging system revealed the two-dimensional intensity distribution of these radiations; for example, oscillating contrast, such as equal thickness contour appears in silicon, and hole edges in a silver thin film show bright fringe contrast due to radiative surface plasmon.

Key Words: Transmission electron microscope, Cherenkov radiation, thin films, particles, surface plasmon, mica, silicon, silver.

*Address for correspondence:
Naoki Yamamoto
Department of Physics,
Tokyo Institute of Technology,
Oh-okayama, Meguro-ku,
Tokyo 152,
Japan

Telephone number: 81-3-5734-2481
FAX number: 81-3-5734-2079

Introduction

It is known that a charged particle can emit light when it moves in transparent medium with a velocity larger than the phase velocity of light; this is called Cherenkov radiation. There is another type of radiation which is generated when a charged particle passes through a boundary between two media with different dielectric constants, which is called transition radiation. Recently, these radiations were detected in transmission electron microscopy (TEM) by a light detection system originally developed for cathodoluminescence (CL) [6].

Specimen thicknesses used for TEM observation are usually less than 1 μm which is comparable with the wavelength of visible light. Some characteristic features are seen in the emission spectra of these radiations due to interference effect, for example, intensity oscillation against wavelength appears in the spectra from dielectric and semiconductor thin films, which depends on specimen thickness and accelerating voltage [5, 7]. In the case of metal thin film, transition radiation is predominant. In addition, the radiative mode of the surface plasmon, called the Ferrell mode, gives rise to a sharp peak in an emission spectrum as a part of the transition radiation field. Such a peak was observed for a silver thin film at the wavelength corresponding to the plasma frequency, and was found to be sensitive to the morphology of the films.

Recently, we have developed an imaging system using the collected light signal, which visualizes the two-dimensional intensity distribution of the radiation. In this paper, we show characteristic features in the emission spectra from thin films of mica and silicon, and monochromatic images of the specimens using emission signal of specific wavelengths. Particles of MgO and $BaTiO_3$ were also studied by this technique.

Emission From Mica Films

Cherenkov radiation generated in a thick medium has the following characteristic properties: (1) threshold of the velocity of electrons or accelerating voltage for its

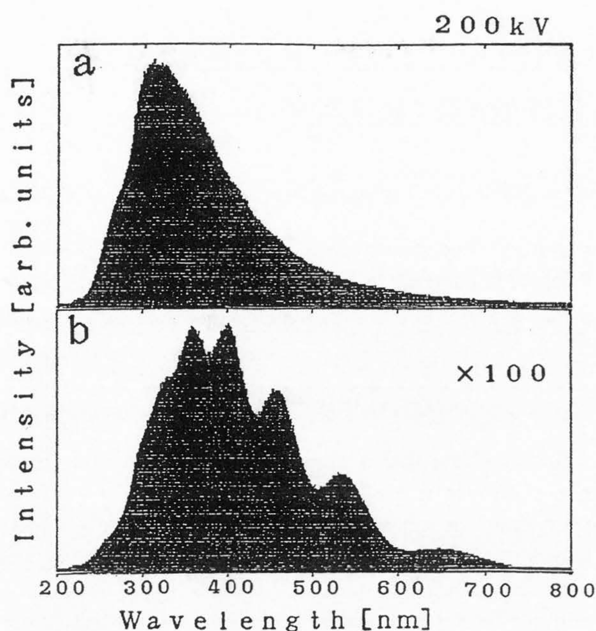

Figure 1. Forward (a), and backward (b) emission spectra from a mica thin film taken at 200 kV.

generation, $v > c/n$, where n is the refractive index of the material; (2) emission angle is given by $\theta = \cos^{-1}(1/n\beta)$ which is less than 90°; (3) spectral shape shows wavelength dependence of λ^{-2}; and (4) intensity is proportional to film thickness. Figures 1a and 1b show observed spectra from a mica film taken at the accelerating voltage of 200 kV. An ellipsoidal mirror is used for light collection, which can be set below or above the specimen in TEM in order to detect forward and backward emission. The spectra in Figures 1a and 1b correspond to the forward and backward emission, respectively. The intensity of the forward emission is stronger than that of the backward one by a factor of 100. The decrease in intensity in the short wavelength range below 300 nm is due to detection deficiency of the system. The forward emission in Figure 1a has the properties of Cherenkov radiation mentioned above. The backward emission shows a set of peaks in the spectrum of Figure 1b, and their positions change with accelerating voltage and film thickness. The peak wavelength λ_m of the m-th order is approximately given by the following relation:

$$(d/\beta)\,(1 + \beta n \cos\theta') = (m + 1/2)\lambda_m, \quad (1)$$

where d is thickness of a specimen; $\beta = v/c$ (v is the velocity of electron); n is the refractive index, $n = 1.59$ for mica; and θ', the emission angle inside the specimen. The observed spectra can be reproduced well by the calculation using the formula derived by Ritchie and Eldridge [4], and Pafomov and Frank [2]. The film thickness can be determined to be 1.20 μm with an accuracy of less than 10 nm. It is not easy to distinguish between Cherenkov radiation and transition radiation in the backward emission spectrum, but it can be said that the contribution of transition radiation is dominant when the accelerating voltage is less than the threshold value, 146 kV for mica.

Figure 2a shows a transmission electron micrograph of a mica thin film. Several surface steps are seen as parallel lines, and broad dark line contrasts across the steps are bend contours. Figures 2b and 2c are emission spectra taken with an electron beam probe located at points marked A and B in Figure 2a. The accelerating voltage is 200 kV and the ellipsoidal mirror for light collection is set above the specimen. By comparing with calculated spectra, the thicknesses at A and B are found to be 950 nm and 1000 nm, respectively. At the wavelength of 340 nm, the spectrum has a minimum (in Fig. 2b) and a maximum (in Fig. 2c); while at 350 nm, the situation is reversed. Figures 2d, 2e and 2f show monochromatic images of the same area as in Figure 2a, taken at the wavelength of 340 nm, 350 nm, and 550 nm, respectively. The terraces are recognized easily since they have different contrasts: the terrace of A is dark (in Fig. 2d) and bright (in Fig. 2e), while the terrace of B is bright (in Fig. 2d) and dark (in Fig. 2e). It is found from the calculation that the emission intensity at any wavelength change sinusoidally with increasing thickness, and the period is proportional to the wavelength as expected from the above equation.

Emission From Silicon Films

Figure 3a shows a (220) dark field TEM image of a silicon thin film in the (111) orientation taken at 200 kV where equal thickness contours are seen. The emission spectrum shown in Figure 3b is for backward emission taken from a flat region of constant thickness. Silicon absorbs light in the visible region, and then the refractive index is complex, $n = n + ik$; the absorption coefficient k is large in the short wavelength region and is small for wavelength longer than 500 nm. A set of peaks appear in the longer wavelength region, which are generated by interference between transition radiations generated at top and bottom surfaces. Then, the spectral shape in this region changes with specimen thickness and accelerating voltage. On the other hand, the spectral shape in the short wavelength region (below 400 nm) does not depend on those parameters, which is the same as the spectrum from a single boundary between vacuum and a bulk silicon crystal. The two peaks are seen at about 280 nm and 360 nm, which correspond to the peaks in the dielectric function of the imaginary part, and are due to the interband transition between the electronic states. The emission does not have the character

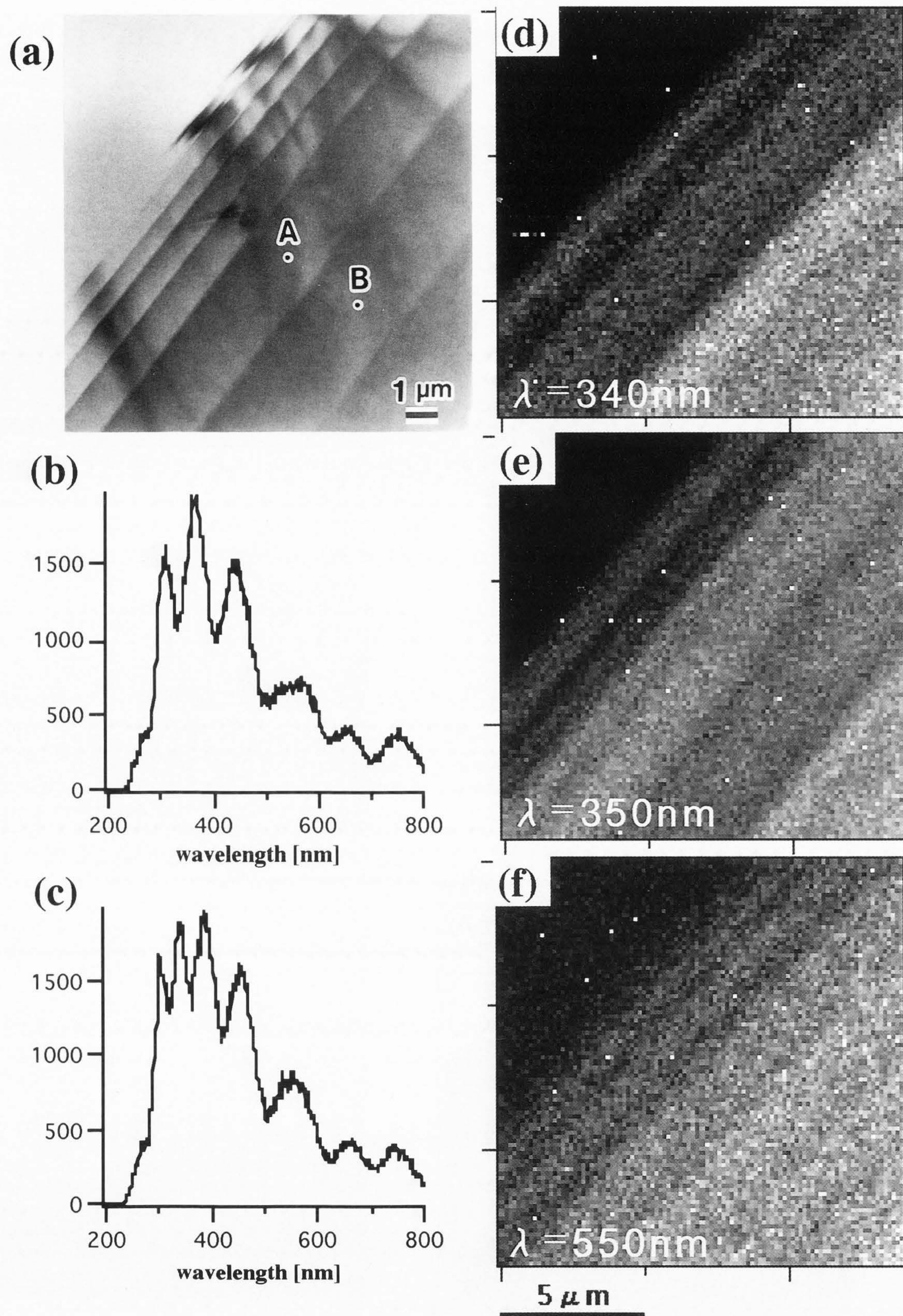

Figure 2. (a) A transmission electron micrograph of thin mica film; (b) and (c) backward emission spectra from the position marked A and B in (a). Monochromatic images of (d) to (f) were taken at the wavelengths of 340 nm, 350 nm, and 550 nm, respectively.

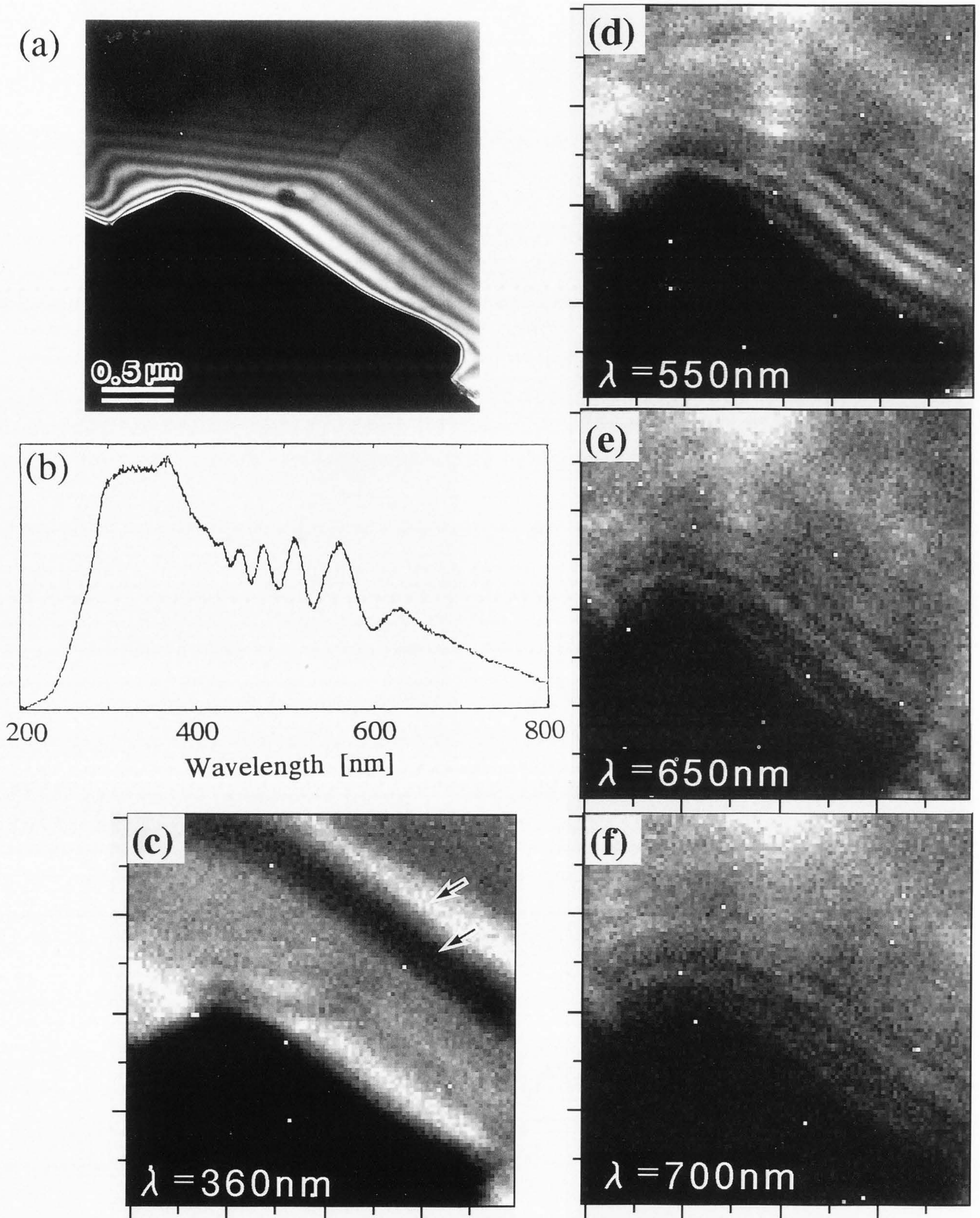

Figure 3. (a) a dark field transmission electron micrograph of Si thin film; (b) a backward emission spectrum from a flat region; and (c) to (f) monochromatic images taken at the wavelengths of 360 nm, 550 nm, 650 nm, and 700 nm, respectively.

of Cherenkov radiation; the intensity is nearly the same for the forward and backward emissions, and does not change with increasing thickness. This is because Cherenkov radiation generated in the specimen is totally reflected by the surfaces because of the large refractive index. Figures 3c to 3f are monochromatic images of the same area as in Figure 3a taken at the wavelengths of 300 nm, 550 nm, 650 nm, and 700 nm, respectively. In Figure 3c, it is seen that a bright contrast appears near the edge and almost uniform contrast arises inside the crystal although the specimen thickness increases there. This feature is in good agreement with the calculated intensity profile shown in Figure 4. However, dark and bright bands are seen in the thicker region as indicated by arrows. These contrasts are not expected from the calculation based on the plate shape specimen at normal incidence. The origin of these contrasts is not clear yet. In Figure 3d, fringe contrasts parallel to the edge are seen corresponding to the equal thickness contour in Figure 3a. The period of the fringes depends on the wavelength of the emission; it increases linearly with the wavelength as seen from Figures 3d to 3f. This feature is well reproduced in the calculated profiles in Figure 4.

Emission From Silver Films

The emissions from metal thin films with thickness less than 100 nm were studied, especially for silver thin films. Transition radiation is dominant in those emissions rather than Cherenkov radiation. The dielectric function of aluminum is a monotonously increasing function of wavelength with a large plasma frequency ($\hbar\omega_p$ = 15 eV), and so the observed emission spectrum from an aluminum film has a simple shape in the optical region, i.e., the intensity monotonously decreases with wavelength. On the other hand, the plasma frequency is small for silver, and the dielectric function of silver has a complicated feature in the optical region. In the backward emission spectrum from a 50 nm thick film of silver, as shown in Figure 5a, a sharp peak is seen to appear at the wavelength of 330 nm which corresponds to the volume plasmon frequency of $\hbar\omega_q$ = 3.78 eV. This peak was not observed in the forward emission, and even in the backward emission, the peak disappeared for the films thicker than 100 nm. The existence of the peak is due to the radiative mode of surface plasmon which was first predicted by Ferrell, so is called "Ferrell mode" [3]. In the emission spectra from an inhomogeneous film containing holes and grains, the peak is immersed in the broad peak with a peak wavelength around 420 nm as shown in Figure 5b. The increment of this broad peak from Figure 5a to 5b is considered to be due to non-radiative mode of surface plasmon which can emits light through surface roughness [1].

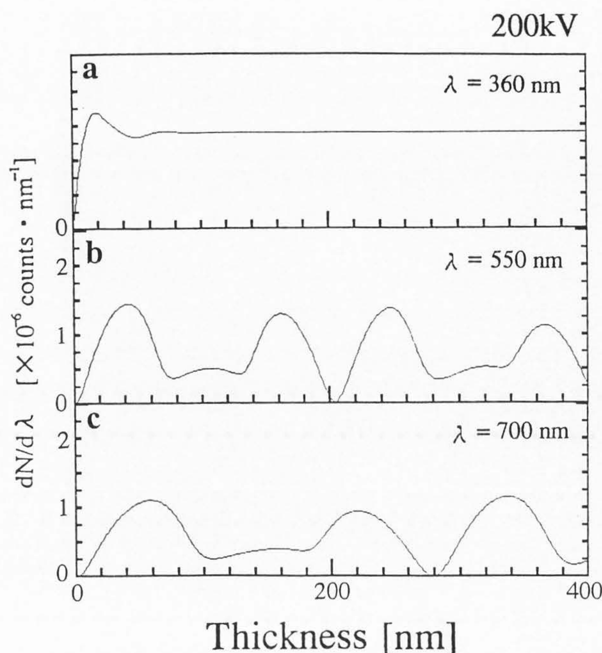

Figure 4. Profiles of emission intensity versus thickness calculated for the wavelengths of (a) 360 nm; (b) 550 nm; and (c) 700 nm.

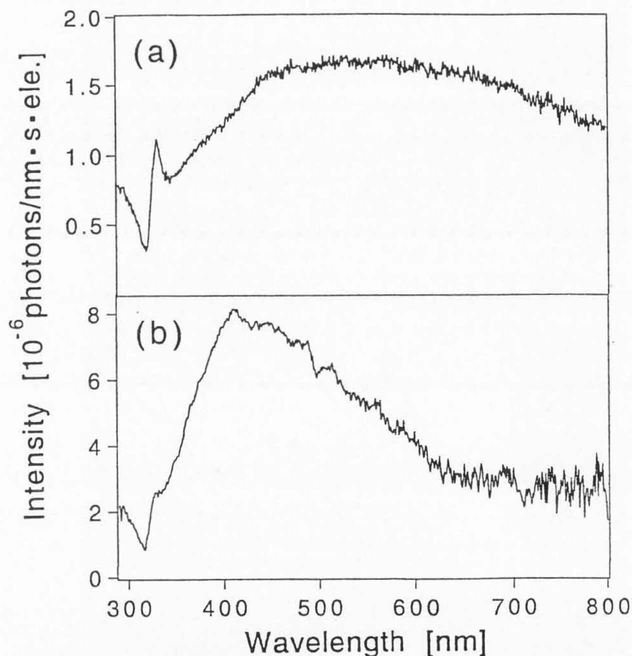

Figure 5. Backward emission spectra from silver thin films of 50 nm thickness taken at 200 kV: (a) a single crystal film; and (b) a film containing holes and slightly misoriented grains.

Monochromatic images using these radiations are shown in Figure 6 where Figure 6a is a scanning electron micrograph of a silver film (50 nm in thickness)

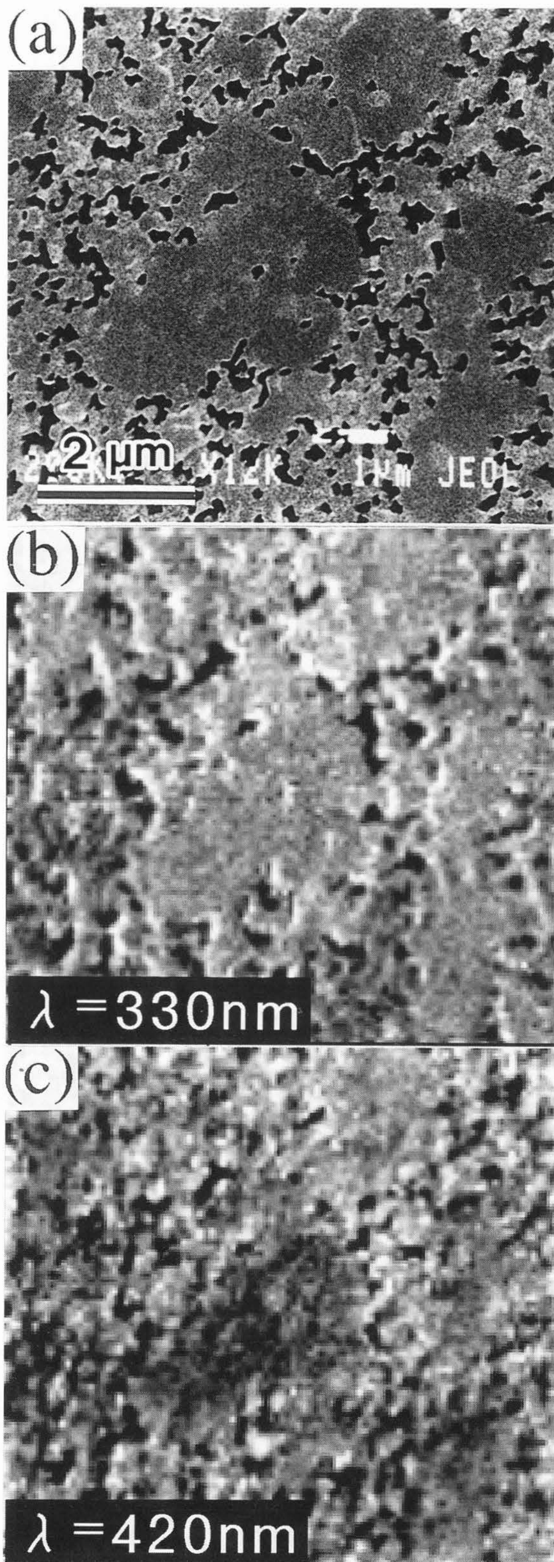

Figure 6. (a) A scanning electron micrograph of the specimen containing holes and grains (Fig. 5b); and (b) and (c) monochromatic images taken at the wavelengths of 330 nm and 420 nm, respectively.

having holes, and Figures 6b and 6c are monochromatic images of the same area taken at 330 nm and 420 nm, respectively. It is seen in Figure 6b that a characteristic bright fringe contrast appears along the edges of the holes, and a rather uniform contrast appears in the inside region apart from the edges, while in Figure 6c, inhomogeneous contrasts are seen to arise both in the inside region and near the hole edges. The latter contrast is considered to reveal the roughness of the film. The resolution of the monochromatic image is about 50 nm as estimated from the image of Figure 6b. The resolution depends on wavelength; the resolution in Figure 6b is slightly better than that in Figure 6c. This is considered to be due to difference in life-time for the radiative and non-radiative surface plasmon modes.

Emission From Particles

Emission spectra from particles of $BaTiO_3$ and MgO were studied. A $BaTiO_3$ plate shows a broad peak near 400 nm and rapid decrease below 400 nm due to absorption. A particle of $BaTiO_3$ with spherical shape shows a similar spectrum with a rather sharp peak, and the peak position moves to short wavelength as a particle size becomes small from 3 μm to 60 nm. A set of peaks due to interference were observed for a particle of diameter around 1 μm.

Figure 7a shows a transmission electron micrograph of a MgO smoke crystal of cube shape in the [100] orientation, and Figures 7b and 7c are forward emission spectra from the crystal taken at 200 kV with the electron beam of a probe size of 0.1 μm located at places marked by white circles 1 and 2 in Figure 7a, respectively. It is found that (as seen in Figs. 7b and 7c) the spectral shape changes remarkably when the beam position shifts on the specimen. The spectrum of Figure 7b has a shape similar to that of mica in Figure 1a, which has a character of Cherenkov radiation. While in the spectrum of Figure 7c, many peaks appears. The peak position changes with particle size, then their appearance is mainly due to interference effect. A backward emission spectrum was also observed in which those peaks are less intense. Very few theoretical works for the radiation from particles has been done so far. The radiation generated by electrons passing near the side surface of the cube should contain Smith-Purcell radiation, and so the interpretation may become more complicated.

References

[1]. Heitmann D (1977) Radiative decay of surface plasmons excited by fast electrons on periodically modulated silver surfaces. J. Phys. C **10**, 397-405.

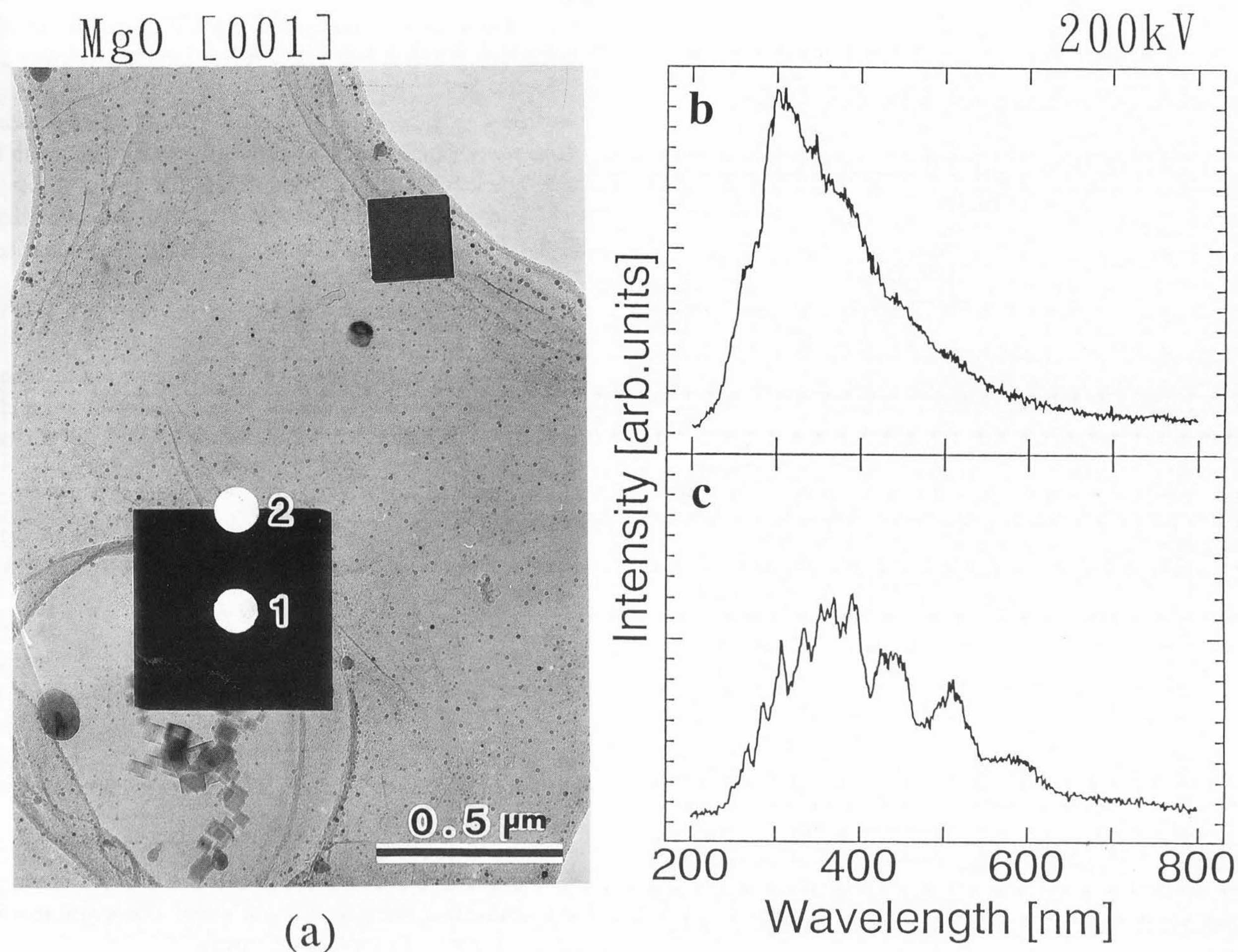

Figure 7. (a) Transmission electron micrograph of a MgO smoke crystal in the [001] orientation; and (b) and (c) forward emission spectra taken with an electron beam located at the positions marked by white circles 1 and 2 in (a).

[2]. Pafomov VE, Frank IM (1967). Transition radiation at two parallel interfaces. Sov. J. Nucl. Phys. **5**, 448-454.

[3]. Raether H (1980) Excitation of Plasmons and Interband Transitions by Electrons. Springer-Verlag, New York. p. 116.

[4]. Ritchie RH, Eldridge HB (1962) Optical emission from irradiated foils. I. Phys. Rev. **126**, 1935-1947.

[5]. Sugiyama H, Toda A, Yamamoto N (1994) Detection of Cherenkov and transition radiation in TEM. Proc. 13th Int. Conf. Electron Microscopy, vol. 1. Les Editions de Physique, Paris. pp. 833-834 (extended abstract).

[6]. Yamamoto N (1990) Characterization of crystal defects by cathodoluminescence detection system combined with TEM. Trans. Jpn. Inst. Metals **31**, 659-665.

[7]. Yamamoto N, Sugiyama H (1991) Cherenkov and transition radiation generated in 200 kV electron microscope. Radiat. Eff. Defects Solids **117**, 5-10.

Discussion with Reviewers

R.H. Ritchie: Can you please furnish more detail about experimental parameters? For example, what is the solid angle subtended by the spectrometer and at what angle was it placed in the experiments reported?

Authors: In our light detection system, an ellipsoidal mirror is used for collecting light emitted from a specimen in a transmission electron microscope. The emitted light is guided outside the TEM through a window and a polarizer, and focused at the spectrometer slit by a concave mirror. The arrangement of the ellipsoidal mirror in TEM is illustrated in Figure 8. The solid angle subtended by the mirror is about 56% of the total solid angle of hemisphere. Then the observed emission spectra are integrated ones over this solid angle, and for the calculation of emission spectra such integration over the subtended solid angle was performed. The electron beam current usually used is of the order of 10 nA with a beam diameter of about 10 nm.

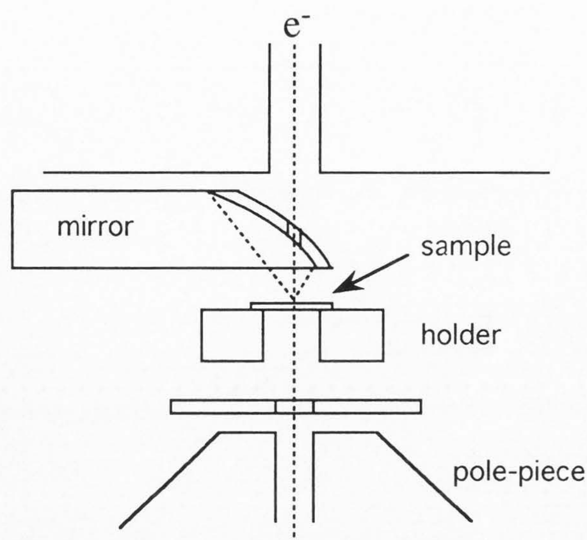

Figure 8. Arrangement for the ellipsoidal mirror.

R.H. Ritchie: The authors suggest that Smith-Purcell radiation should be contained in the radiation field emitted in the passage of fast electrons parallel to the side surfaces of MgO cubes thus complicating the interpretation of the observations. It should be noted that such radiation from the crystal structure of the cubes is expected to lie in the X-ray region, with wavelengths of the order of the crystal spacing, and thus should not interfere with the Cherenkov or transition radiation fields.

Authors: The wavelength of Smith-Purcell radiation is given as $\lambda = \{D(1/\beta - \cos\theta)\}$ where D is a grating period along an electron path and θ an emission angle. If D is regarded as a period of surface steps in the side surface, having a magnitude of an order of 0.1 μm, the radiation can arise in the optical region. However, in the case of the MgO cubic crystal, the intensity of this radiation is expected to be weak, since the number of steps is very small if they exist, and the material is not metal. Another contribution to the emission is also considered, that is a radiation produced by a lateral acceleration of electrons by the potential of the cube edge, though it might have a wavelength in the ultra-violet (UV) region. A major factor to change in spectral shape in Figure 7 is considered to be the interference effect inside the cube. However, the emission generated at the position 2 in Figure 7 near the side surface is not the same as that generated at the position 1; in the latter case the emission is similar to that of a plate-shaped specimen. This also makes it difficult to interpret the result.

R. Vincent: A threshold of 146 kV is quoted for the emission of transition radiation from mica; how was this calculated?

Authors: This value is the threshold accelerating voltage of Cherenkov radiation for mica, which can be generated under the condition that $v > c/n$ or $\beta n > 1$, where n is the refractive index. Then, the threshold voltage V_{sh} is readily given by the following equation:

$$eV_{sh} = mc^2 \{(1-\beta^2)^{-1/2} - 1\}$$

with $\beta = 1/n$ and $mc^2 = 511$ keV. Below the threshold voltage, the contribution of Cherenkov radiation rapidly decreases, and that of the transition radiation becomes dominant.

R. Vincent: In Figure 6b, the distribution of light emitted around the edges of holes is evidently asymmetric. Is this an artifact of the CL detection optics?

Authors: Yes. The angular distribution of the light collection by the ellipsoidal mirror does not have an axial symmetry about the electron incident direction, as seen in Figure 8 (arrangement of the mirror). This gives such asymmetry in the fringe contrast along the edge of the hole where the angular distribution of the emission has a special directionality.

R. Vincent: More generally, do the authors envisage any immediate application of their observations for microanalysis of metallic specimens?

Authors: The method mentioned here uses Cherenkov radiation and transition radiation, both of which depend on the dielectric constant of material. Thus, this method may become important in investigating the local dielectric properties of inhomogeneous materials with a high spatial resolution. At present, we are applying this method to visualize a localized silicon oxide thin film on a silicon substrate and metal islands on semiconductor substrates. There should be many other applications of this method; the observation of the microstructures in metals and alloys is also an interesting application.